Control of Free-Radical Emulsion Polymerization of Methyl Methacrylate by Oxygen Injection. II. Experimental Study

BRIAN M. LOUIE, THOMAS FRANASZEK, TINA PHO, WEN YEN CHIU, and DAVID S. SOONG, *Department of Chemical Engineering, University of California, Berkeley, California 94720*

Synopsis

Oxygen injection has been proposed and experimentally demonstrated as an effective control measure for limiting the rate of heat release and altering the rate of polymerization in emulsion processes. A detailed mathematical model has been previously developed to describe the system behavior with and without oxygen injection. A simple lab scale apparatus was constructed and run extensively. Only trace quantities of oxygen are needed to inhibit the reaction completely. The facile response makes this method attractive for fast temperature control. However, because of the rapid penetration of dissolved oxygen into the polymer particles, growing radical chains are terminated prematurely, lowering product molecular weights. To minimize this detrimental effect, pulsed oxygen control is used and extensive experimental work was performed to determine the effects of controller set points on molecular weight. Moderate oxygen flows and moderate set point temperatures are found to give the optimal response without significant lowering of the final molecular weight. Injected quantities agree well with the order-of-magnitude sparging calculations needed to completely stop initiation. However, complete agreement between model simulations and experimental results was not reached due to an unmeasured loss of monomer from the reactor. Chain transfer to monomer is found to be important in modeling the polymer molecular weight. It has, however, a negligible effect on the reaction rate.

INTRODUCTION

In Part I of this two-part series investigating the idea of using pulsed oxygen injection to curb excessive temperature rises in a methyl methacrylate emulsion polymerization reactor, we conducted a detailed modeling study based on a recently published gel-effect model from this laboratory. Results of this effort indicated that this proposed control strategy may indeed be promising; we now carry out preliminary experiments to verify the feasibility of this proposal and to characterize the polymers produced in the presence of oxygen.

EXPERIMENTAL APPARATUS

The apparatus shown in Figure 1 was used to gather batch experimental data with and without oxygen control. An agitated 1-L three-necked distillation flask was used as the reactor. Two reflux condensers and an agitator shaft water seal were used to prevent the loss of monomer and water from the reactor. Agitation was provided by a Talboy Model 120, 1/75 HP stirrer with a polypropylene marine-type impeller. A 1-gal water bath was used

Journal of Applied Polymer Science, Vol. 30, 3841–3856 (1985)
 CCC 0021-8995/85/093841-16$04.00

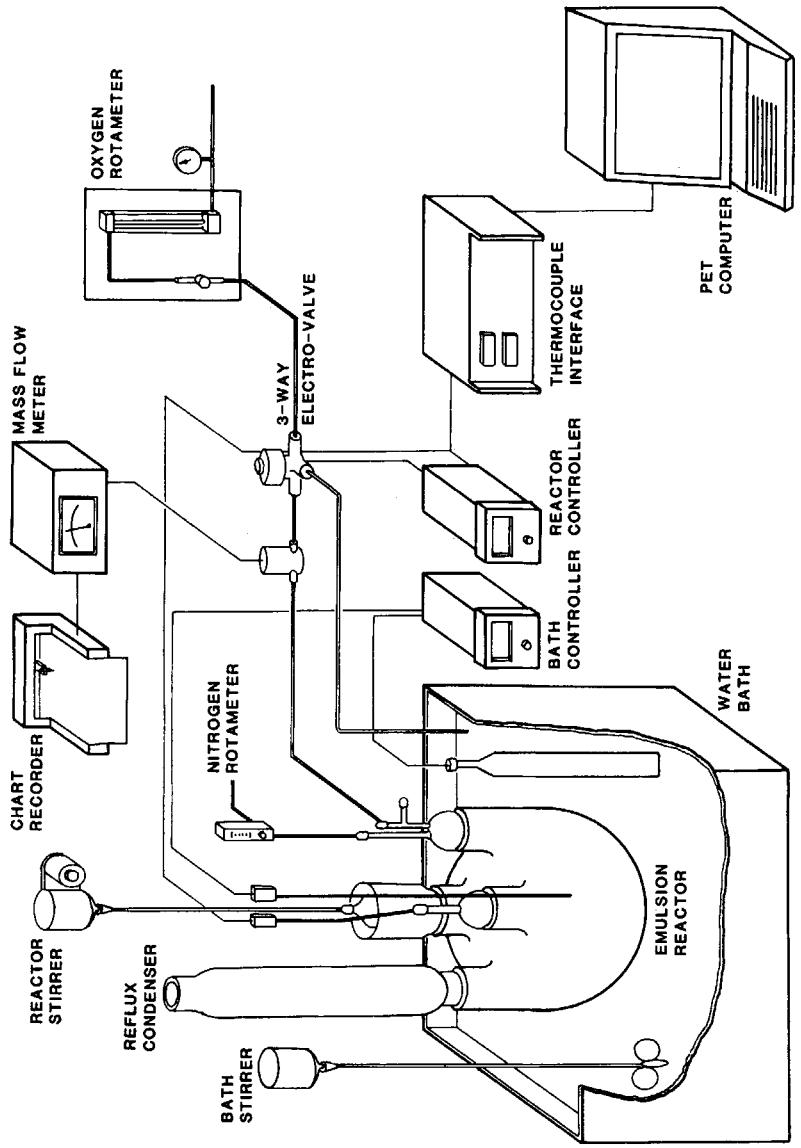

Fig. 1. Pictorial representation of the experimental emulsion polymerization apparatus used for selective oxygen injection. (A second in-line condenser, heating blade, and disk drive have not been shown, for clarity.)

as a constant temperature, cooling jacket at the initial reaction temperature. Bath temperature was regulated by a Model DIC Shinko PI controller and heat provided by two 250-W blade heaters.

A nitrogen flow, at about 10 standard cubic feet per hour (SCFH), provided an inert atmosphere over the liquid content. Oxygen flow was first metered through a Matheson R7640 Series Rotameter with a no. 610 tube. The reading here was referred to as the maximum flow rate, prior to the controller intervention. It then flowed to through an ASCO ¼-in. solenoid operated, three-way valve, controlled by an Omega Model 157-718 PID controller operated in proportional mode. When the valve was closed, oxygen was vented into the water bath. When the valve was open, oxygen flowed into the reactor. The actual oxygen delivery rate to the reactor was measured by a Matheson Model 8110-0251 Mass Flow Meter and recorded on a strip chart recorder. Both reactor and bath temperature were monitored with a pair of Analog Devices Digital Thermometers #AD2036, interfaced with a Commodore Series 2001 PET minicomputer and Model 4040 dual disk drive for data storage.

Methyl methacrylate monomer with 60 ppm monomethyl hydroquinone inhibitor was obtained from Aldrich Chemical Co. Reduced pressure distillation (at 26 in Hg or " Hg vacuum and 45°C) was initially used to remove the inhibitor for batch experiments. However, because of the extremely low distillation rates (1 mL/min) in our still, later experiments (those with oxygen control) used monomer which had been purified by passing the MMA through a bed of Amberlyst A-27 ion exchange resin (Rohm and Haas Chemical Co.). Duplicate tests showed no difference in the rate of polymerization between distilled and purified MMA. Reagent grade sodium lauryl sulfate (dodecyl sodium sulfate) emulsifier was obtained from MCB Manufacturing Chemists. Potassium persulfate initiator was obtained from Mallinckrodt, also in reagent grade. In-house distilled water, nitrogen, and oxygen were used.

The experimental conditions are given in Table I. Conditions 1 and 2 used 6 mol MMA/L water while conditions 3 and 4 used 10 mol MMA/L water, the maximum monomer loading. Condition 2 was taken as the base experimental condition for oxygen control. Agitation speed was not important as long as the emulsion is well mixed.[1] Our stirrer speed was in the neighborhood of 500 rpm.

At the beginning of an experiment, the water bath was brought to the desired temperature. The condenser cooling water flow rate was then adjusted to the range 850–950 mL/min to ensure adequate cooling. The MMA, water, and surfactant were then added, and the nitrogen blanket was start-

TABLE I
Experimental Operating Conditions for the Emulsion Polymerization of MMA

Condition	T (°C)	[M] (g/L H_2O)	[I] (g/L H_2O)	[S] (g/L H_2O)
1	50	600	1	10
2	60	600	1	10
3	50	1000	1	10
4	60	1000	1	10

ed. The maximum oxygen flow was set, and visual sighting of bubbles was obtained prior to adjusting the set point of the oxygen controller. The oxygen injection line was then clamped just above the reactor to prevent back contamination from dissolved nitrogen in the liquid and premature oxygen addition. Agitation was then started. After about 35 min, the initiator was added in powder form to begin the polymerization. A little more water (1–5 mL) was used to wash any remaining initiator clinging to the sides of the opening into the reactor. This tedious startup procedure and the long startup time allowed the system to equilibrate thermally and the last traces of dissolved O_2 to be removed by nitrogen stripping.

A 10 mL sample was withdrawn from the reactor every 2.5 min with a syringe and poured into a preweighed sample bottle containing about 10 mL of toluene and trace quantities of DPPH inhibitor (Polysciences). The sample was then cooled in ice and mixed with excess methanol to precipitate product PMMA. Evaporation of the unused monomer, water, and methanol occurred in a fume hood until dry. The residual solid was then vacuumed to removed any remaining moisture. The conversion was then determined gravimetrically. Selected samples were next dissolved in methyl ethyl ketone (2-butanone), and the molecular weight determined by viscometry with a Ubbelohde OB viscometer (Cannon Instruments). The viscosity average molecular weight was determined from the intrinsic viscosity by[2]

$$[\eta] = 9.39 \times 10^{-3}\, \overline{M}_v^{0.65} \quad \text{(mL/g)} \quad \text{at } 25°\text{C}$$

for $\overline{M}_v$ between 16×10^4 to 910×10^4 g/mol. All solvents used in sample handling were obtained from Mallinckrodt, in reagent grade.

RESULTS AND DISCUSSION

Typical experimental temperature and conversion histories are shown in Figures 2 and 3 for conditions 1–3. Nine uncontrolled experiments were conducted on the four conditions listed in Table I to test the reproducibility of our experimental results. Only one run was performed on condition 4 because the emulsion boiled out of the reactor from the larger amount of heat released. The boiling point of the emulsion could be determined from the boiling point of an immiscible mixture of two components (MMA and water) similar to calculations of steam distillation using Raoult's law.

Because of the evaporation of small quantities of water in the reactor, a 1°C temperature difference exists between the bath and the reactor. This difference is quickly overcome as soon as the reaction begins. Since the bath temperature never rises more than 1°C above the initial temperature during an experiment (even at high monomer loadings), the bath temperature has not been shown in all figures, for the sake of clarity. The reactor temperature rises steadily until the onset of the gel effect, where it rapidly increases (see Figs. 2 and 3). The maximum temperature is soon reached, and the temperature falls as the reaction approaches completion. A maximum temperature rise of 2°C is seen for condition 1, while rises of more than 15°C occurs in conditions 3 and 4. Conversion also increases steadily with time and accelerates during the gel effect. A limiting conversion is

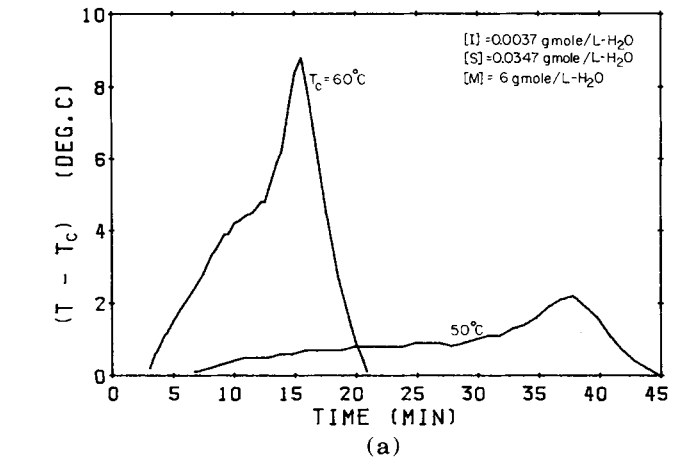

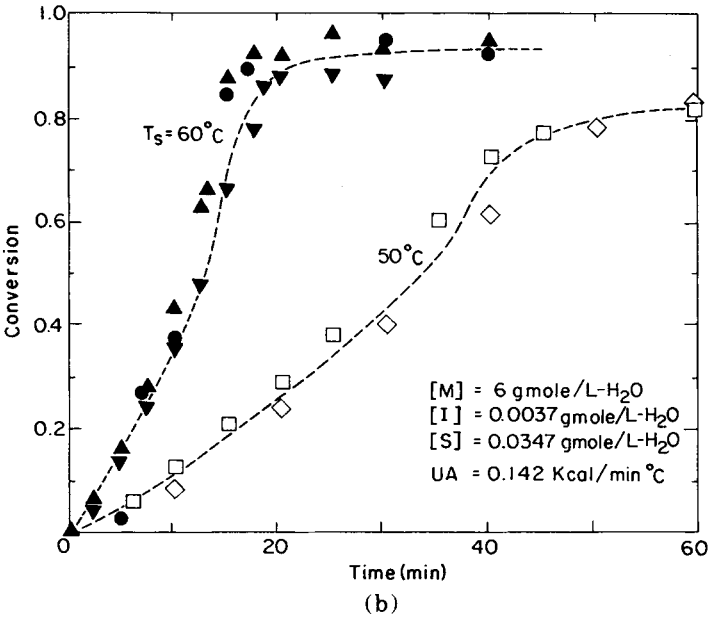

Fig. 2. Nonisothermal emulsion polymerization of MMA. Influence of the coolant temperature on the experimental reactor temperature and monomer conversion.

soon reached as the glass effect occurs. Most of the experimental error in determining the conversion could be attributed to incomplete removal of the last traces of moisture from a sample prior to weighing. A smaller error was introduced in sample transfer from the sample bottle to a drying beaker. Any polymer left on the walls would decrease the apparent conversion. Errors were minimized by vacuum drying and scrupulously rinsing the walls of the sample bottles. Reported conversions are in error by at most 5%.

Figure 2 shows the experimental results for a change in initial temperature. As expected, a much higher temperature rise occurs at the higher bath temperature. The faster reaction rates release the heat of polymer-

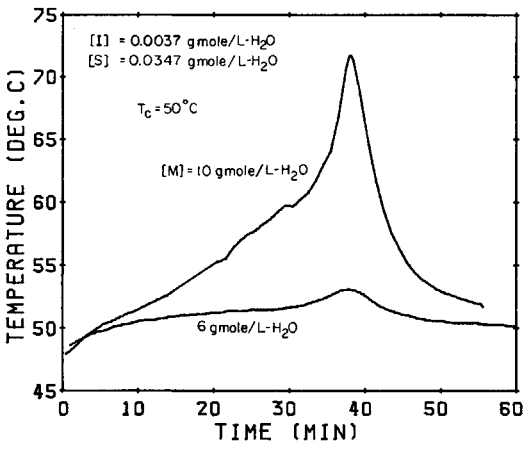

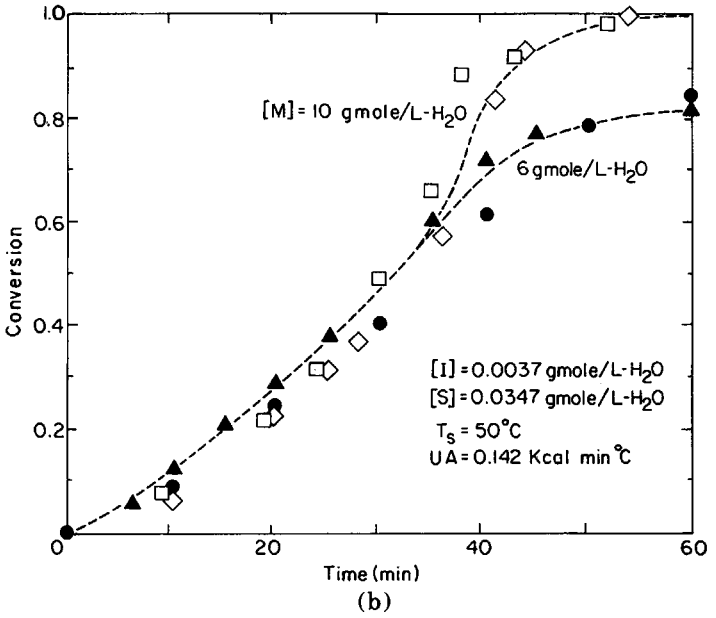

Fig. 3. Nonisothermal emulsion polymerization of MMA. Influence of monomer loading on the experimental reactor temperature and monomer conversion.

ization more rapidly. Figure 3 shows the effect of varying the monomer loading in the emulsion formulation. Much more heat is released in the reactor with 10 mol MMA/L water than 6 mol MMA/L water. This strong temperature rise apparently consumes the extra monomer and allows for complete conversion as the temperature inside the polymer particles rises above the glass transition temperature of PMMA, eliminating the potential glass effect which would otherwise restrict complete monomer conversion.

Careful comparison of Figure 2 (curve 1) of Part I and Figure 2 here shows that experimental rates are much faster than theoretical polymerization

rates. In addition, Figure 3 reveals that 10 mol MMA/L H_2O can be consumed in almost the same time as 6 mol MMA/L H_2O. This is mainly possible because of the hotter temperatures encountered during the polymerization with the higher monomer loading. However, simulated results shown in Figures 2 and 6 of Part I suggest that more time should have been needed to polymerize the extra monomer, even after accounting for nonisothermal behavior.

These discrepancies were initially thought to be attributable to either using the wrong rate of initiation or inaccurately measuring the overall heat transfer coefficient of the lab reactor. Figure 4 shows the spread of literature data on the decomposition rate constant of potassium persulfate with the correlation used in our model. Gardon[1] justified using faster rate constants in modeling the polymerization due to pH changes which occurred during the reaction. However, Kolthoff and Miller[3] reported that the acid catalyzed reaction did not produce more free radicals, consistent with the mechanism below:

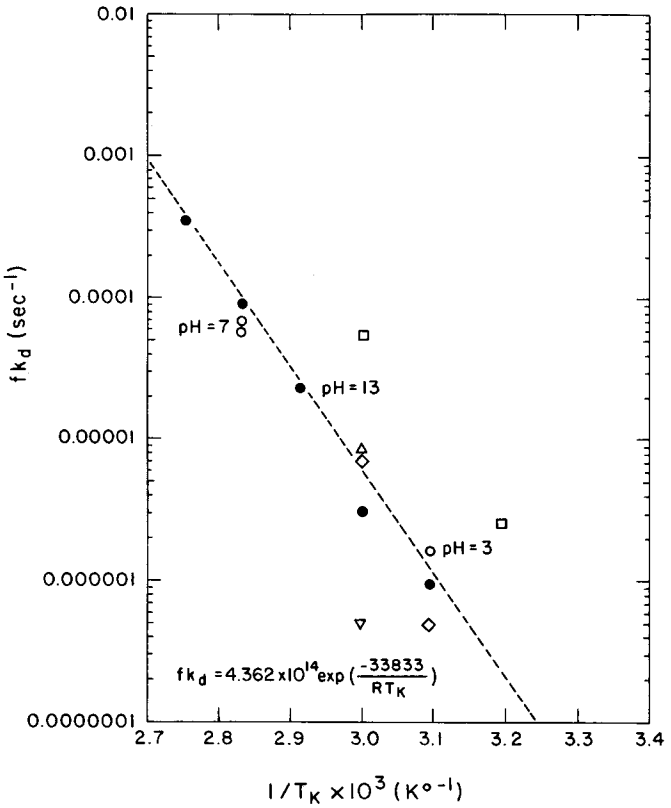

Fig. 4. Reported thermal decomposition rate constants for potassium persulfate. Notice the wide spread of the data. pH appears to have a minor effect (our experimental pH was 6). Data sources: (□) Gardon[1]; (○, ●) *Polymer Handbook*[2] (f = 1.0); (◇) Friis and Hamielec[5]; (△) Patsiga, et al.[6]; (▽) Lynch and Kiparissides[7].

$$S_2O_8^{-2} + H^+ \rightarrow HS_2O_8^- \rightarrow SO_4 + HSO_4^-$$

$$SO_4 + H_2O \rightarrow H_2SO_5$$

$$SO_4 \rightarrow SO_3 + \frac{1}{2}O_2$$

$$SO_3 + H_2O \rightarrow H_2SO_4$$

In addition, we tested the pH before and after several experiments and found no noticeable change in pH. The heat transfer coefficient was remeasured by following the system response curve to a step change in the surrounding temperature in the absence of reaction. A value similar to the original number used in the model simulation was obtained.

After these possibilities were eliminated, the discrepancies between the data and the simulation could then only be reconciled by assuming a loss of monomer had occurred. Figure 5 shows that good agreement between the conversion and temperature profiles can be obtained once the monomer

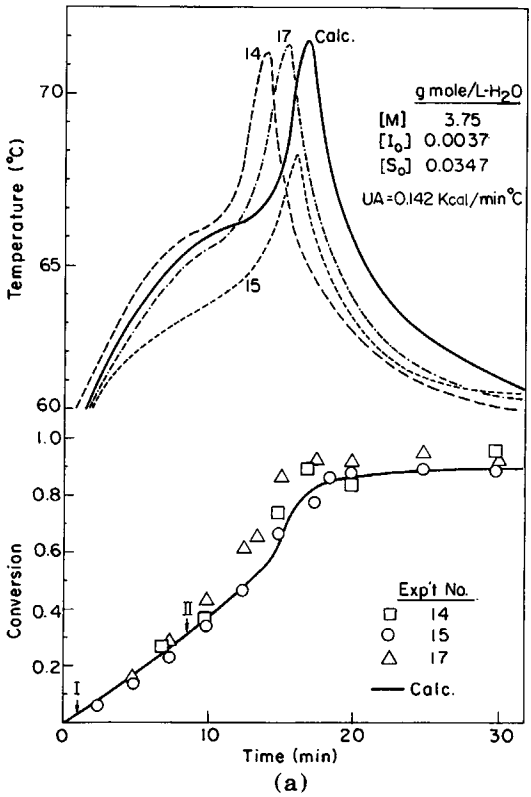

Fig. 5. Comparison of the experimental conversion, viscosity average MW, and temperature histories with model predictions. (The monomer concentration needed to be adjusted to bring the model into agreement—implying that a loss of monomer occurred during our experiments.) (□) Expt 14 and (○) expt 15 (M_v data); (— — —) M_n calcd and (— + —) M_w calcd (CTA = 1.0).

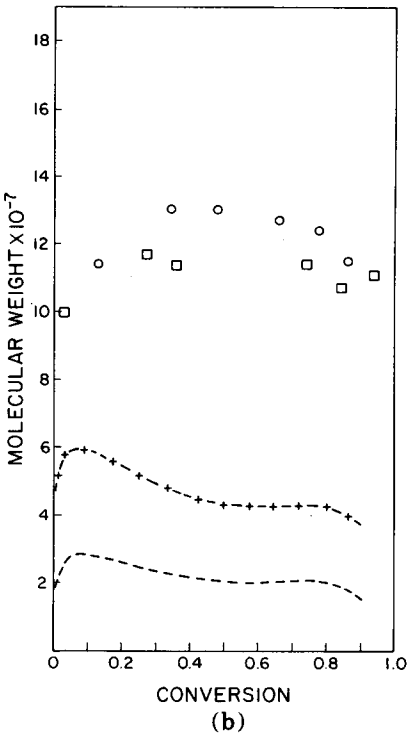

Fig. 5. *(continued from previous page)*

loading is adjusted. This supports the hypothesis that a loss of monomer (from 6 g mol/L H_2O to 3.75 g mol/L H_2O) had occurred in our experiments. It is unfortunate that this problem was not detected earlier and corrected. Nitrogen gas used to blanket the reactor probably swept out the missing MMA during the period prior to adding the initiator. Reproducible results were still obtained since the same procedure was precisely duplicated each time for a given experimental condition. MW predictions are not significantly affected by changes in monomer loading (see Fig. 6 of Part I).

Experimental MWs are much higher than those predicted by the simulation assuming $\overline{M}_v \simeq \overline{M}_w$ (usually $\overline{M}_n < \overline{M}_v < \overline{M}_w$). This might have been due to the loss of significant amounts of water as higher surfactant loadings tends to increase MW faster than higher initiator concentrations (refer to Fig. 2 of Part I for the effect of doubling either S and I while holding the other constant). However, water is less volatile than MMA and is thus preferentially returned to the reactor by the reflux condensers. In addition, almost half of the water added to the reactor originally must be removed to account for the difference in MW. Since such a loss would not go unnoticed, it is unlikely that the discrepancy between the MW predictions is due to a loss of water.

The difference between the MW data and the simulation is then most likely due to the inherent inaccurancy of measuring polymer MW by viscometry. James and Piirma[4] demonstrated that a 40% error could occur

by using different correlations for the same intrinsic viscosity data. They also found that the calculated viscosity average MW was larger than the weight average MW as determined by GPC analysis. This is consistent with our results. Efforts to determine MW and MWD by GPC techniques failed, due to plugging of our GPC columns by the large size of the molecules.

Figures 6 and 7 contrast results of two oxygen control runs (runs 31 and 42) with the corresponding uncontrolled run (run 14 or run 15). An oxygen control run is affected by two important variables: (1) the set point temperature and (2) the maximum oxygen flow rate. By varying the maximum O_2 flow rate, the actual controller gain can be varied. The set point temperature determines when to begin oxygen injection. Run 42 used a tem-

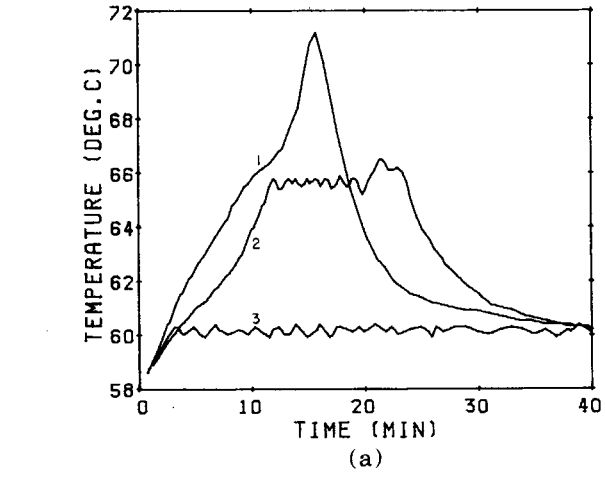

(a)

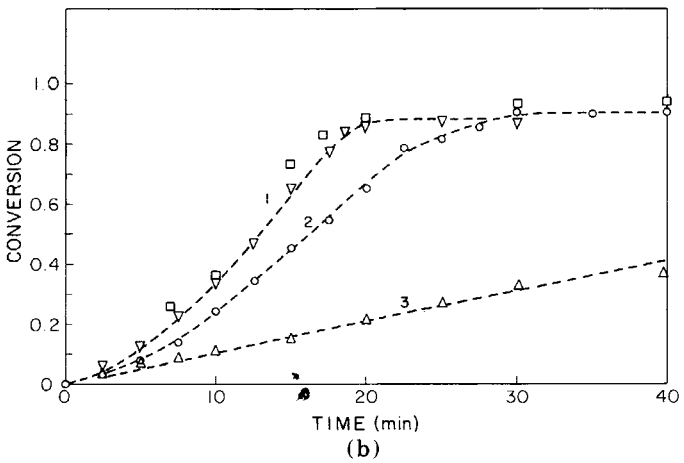

(b)

Fig. 6. Comparison of experimental temperature and conversion histories with and without oxygen control: (1) uncontrolled base case (runs 14 and 15); (2) oxygen control with T_{set} = 68°C and max O_2 flow of 40 sccm (run 42); (3) oxygen control with T_{set} = 62°C and max O_2 flow of 50 sccm. Emulsion runs: (○) 42; (△) 31; (▽) 15; (□) 14.

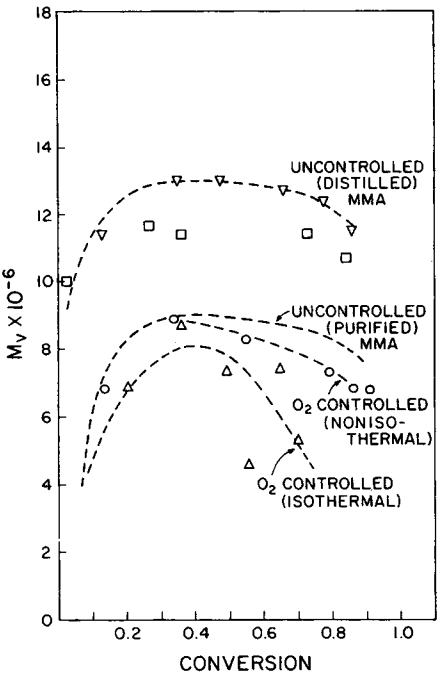

Fig. 7. Influence of monomer purification technique and oxygen control on the experimental viscosity average molecular weight on the nonisothermal emulsion polymerization of MMA. Emulsion runs: (□) 14; (▽) 15; (○) 42; (△) 31.

perature set point of 68°C with a maximum O_2 flow of 40 sccm, while run 31 had a 60°C set point with a 55 sccm flow rate. Delivered oxygen rapidly dispersed throughout the reactor and equilibrated between the aqueous phase and the particles. As soon as the oxygen was added, the temperature began to fall. Since near-isothermal control was possible, both aqueous phase primary radicals and macroradicals inside the polymer particles must have been effectively inhibited by the small quantities of oxygen used. This justifies our previous hypothesis that oxygen diffusion and radical deactivation are both very fast processes.

Action was taken by the Omega temperature controller when the reactor temperature rose above a 2° bandwidth around the set point. The solenoid valve was then opened and a small pulse of oxygen injected into the reactor (see Figs. 6 and 8 for run 42). After a few seconds, the temperature was again measured, and a decision was made whether to add another longer or shorter oxygen pulse. The quantity of oxygen delivered per pulse is related to the maximum oxygen flow rate. If the reactor temperature rose above the bandwidth, a continuous stream of oxygen was added. When the temperature fell below the bandwidth, no oxygen was injected. In many cases, the reaction could be stopped with the initial oxygen pulse. Reactor temperature then remained at the lower boundary of the bandwidth with periodic oxygen pulses used to check any temperature rises. Upon comple-

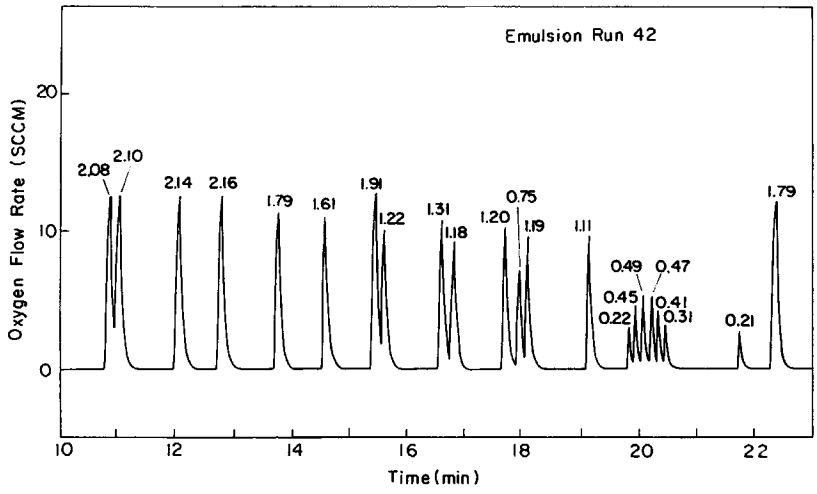

Fig. 8. Typical experimental oxygen injection trace obtained during an oxygen temperature control run. No oxygen is added prior to 10 and after 23 min. Quantities above each peak corresponds to the amounts of oxygen delivered (cm^3).

tion of the polymerization, the temperature rapidly fell back to the surrounding bath temperature.

The importance of trace impurities on the polymer molecular weight can be seen in Figure 7. Molecular weights can differ by as much as 10% for two runs which had almost identical conversion histories (compare runs 14 and 15 in Figs. 6 and 7). In both runs, the monomer had been distilled prior to use. A bigger difference in MW is due to the type of purification treatment used to remove impurities from the MMA (compare initial MWs in runs 31 and 42 with run 15 in Fig. 7). Monomer was primarily distilled to remove inhibitors, but absorption of impurities through a packed bed was more convenient and reportedly just as efficient. However, chain transfering oligomers, originally present in the monomer, can be separated by distillation, but not by absorption. These small impurities passed through the resin bed and lowered MW by about 30%. This effect is so dramatic that scrupulous monomer purification may be required when very high MW is essential (as when PMMA is used as a photoresist material).

The effect of oxygen injection on the polymer MW can then be seen in Figure 7. Very high product MWs are obtained without any temperature control. Oxygen injection lowers the final MW. Shorter chains are produced from the sudden chain termination of live radicals when oxygen is introduced into the reactor. By adding the oxygen earlier into the polymerization, more low MW polymer is formed. This adversely affects the cumulative MW. Reaction times are also prolonged as the number of live radicals is reduced. The lowest MWs with the longest reaction times are found under near-isothermal conditions when oxygen is added at the very beginning to curb the temperature rise. Polymer PD is also likely to significantly increase, as indicated by the large shifts in viscosity average MW. From these

results, we can conclude that *continuous* oxygen addition is *not* a good injection scheme and that some kind of on-off strategy (bang-bang control) is probably better.

A direct comparison with model simulation is not possible for several reasons, First, experimental oxygen flows were more like on-off control rather than strictly proportional control. Second, the equivalent controller gain is not known since the actual dissolved oxygen concentration could not be measured. (The actual controller gain depends on both the maximum O_2 flow rate and the length of a pulse.) Lastly, the experimental and model simulation set points do not correspond to each other as the reaction was controlled by the controller bandwidth. This last point can be circumvented by using a 2° lower set point in the model.

Even if a direct comparison is not possible, indirect comparison of the simulation with a similar experimental condition can be made. Figure 8 shows the experimental oxygen addition profile of run 42. Much of the oxygen was added as sharp pulses during the time the temperature was near the edge of the controller bandwidth. If these pulses are averaged over this time interval, the delivered oxygen flow rate is approximately 2 mL/min. From curve 3 in Figure 11 of Part I, a minimum oxygen flow rate of 0.8 mL/min is needed to obtain a similar conversion and temperature history. These values are in excellent agreement with the computed estimates for the minimum and the theoretical flow rates needed to inhibit the rate of radical initiation as discussed in Part I. The difference in the actual values is due to the higher temperature encountered in run 42 (5°C higher) and the uncertainty of k_L and d_b used in the calculations. Hence, while sparger design is definitely needed if the actual oxygen injection rates are needed, a conservative estimate may be obtained by multiplying the minimum oxygen flow rate by a factor of 10.

A series of sixteen oxygen control experiments have been completed using condition 2 as the base case. Set point temperatures ranged from 66 to 72°C while the maximum oxygen flow rate varied from 5 to 55 sccm. All possible experimental combinations of controller set points and oxygen flow rates can then be displayed on a 2-dimensional grid (see Fig. 11). The majority of the oxygen control experiments were performed along the boundary separating complete control and incomplete suppression of gel effect (as measured by the associated temperature rise). This region of controller and oxygen flow settings is of practical interest, as too much O_2 flow is detrimental to MW while inadequate control leads to heat transfer problems. However, defining the boundary must be done experimentally as the simulation is not accurate enough to guide the actual controller settings.

Figures 9 and 10 qualitatively illustrate the wide range of temperature and conversion profiles experimentally observed. At high temperature set points and low oxygen flow rates, the reaction was not inhibited sufficiently. Temperature profiles looked very similar to an uncontrolled run. A sudden rise in monomer conversion again characterized the conversion histories. When the maximum oxygen flow rate was increased, the sudden temperature rise due to the gel effect was clipped out. Conversion histories still rose upward due to partial retention of the gel effect, but some of the sharpness has been smoothed out. At even higher oxygen flow rates, two

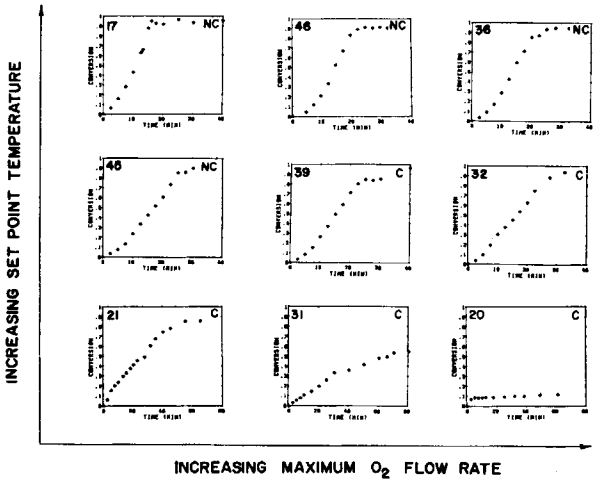

Fig. 9. Proportional temperature control with selective oxygen injection. Schematic representation of the influence of the set point temperature and maximum oxygen flow rate on the experimental monomer conversion. Run numbers in the upper left hand corner correspond to experimental conditions described in Figure 11. Symbols in the upper right hand corner indicate whether the gel effect was controlled (C) or uncontrolled (NC) during the run.

temperature peaks were seen, as more than enough oxygen was injected into the reactor. The entire reaction was stopped and the temperature fell until the last traces of O_2 left by nitrogen stripping (via the N_2 blanket). Temperature then rose as the polymerization resumed. Temperatures again fell as the reaction ended. Conversion profiles exhibited an inflection (and sometimes an initial plateau) prior to reaching the final conversion; this plateau conversion depended on the set point temperature used. Conversion climbed to the limiting (glass) values when the reaction restarted, corresponding to the second temperature spike.

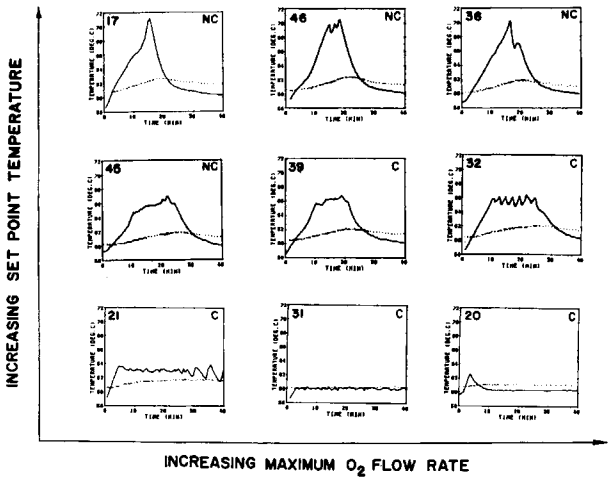

Fig. 10. Proportional temperature control with selective oxygen injection. Schematic representation of the influence of the set point temperature and maximum oxygen flow rate on the experimental reactor temperature. Run numbers correspond to experimental conditions described in Figure 11.

At moderate set points and low flow rates, temperature rose quickly until the lower bandwidth temperature was reached. Oxygen injection effectively checked the temperature rise. Periodic pulses maintained temperature control. Onset of gel effect again marked the start of another temperature rise. Near continuous oxygen injection conditions were used to minimze the gel effect. Conversion profiles resembled those of constant rate curves. Slightly longer batch times were needed due to the lower rates encountered at high conversions. When the maximum flow rate setting was increased, the gel effect was controlled and temperature remained at the lower bandwidth temperature. At still higher maximum oxygen flow rates, temperature again rose to the lower bandwidth temperature, but significant cycling of the reactor temperature occurred with each oxygen injection. Temperature fell several degrees with each oxygen pulse and rose only when all the oxygen was consumed or stripped off.

At low temperature set points and low flows, much longer reaction times were needed to complete a batch. Near isothermal temperature control was possible for most of the run, but small oscillations occurred at the end. Only periodic oxygen addition was needed at the beginning; however, the frequency of the oxygen pulses increased during the gel effect. Conversion histories were characterized by a sudden decrease in reaction rate upon reaching the set point temperature. Batch times significantly increased as the maximum flow rate was increased. At high flow rates, it was possible to completely inhibit the reaction for long periods of time. Reaction temperature increased only after the dissolved oxygen content had been greatly reduced via nitrogen stripping by the N_2 blanket.

Figure 11 shows the effect of set point and maximum O_2 flow rates on the product MW. The highest MWs are obtained under either uncontrolled conditions or high temperature set points. This minimizes the amount of oxygen added into the reactor. Polymer MWs decrease with decreasing temperature set points or increasing maximum oxygen flow rates. The lowest MWs are produced under near isothermal conditions (low set points) and high oxygen flow rates. Hence, injecting too much oxygen has a very strong effect on the final MW. The optimum controller settings appear to be in the range of moderate oxygen flows and intermediate set points (runs 39, 40 or 42). Lower temperatures can only be obtained at the expense of lower MWs under oxygen control. The exact optimum will depend on the reactor cooling system and the minimum tolerable MW. This aspect of oxygen control, i.e., molecular weight reduction, limits its applicability to batch systems.

CONCLUSION

In summary, the feasibility of selective oxygen injection as a control measure for emulsion polymerization processes has been experimentally studied and mathematically modeled. Oxygen injection has been demonstrated as an effective means for curbing the gel effect and manipulating the system temperature. Both controlled and uncontrolled conditions have been simulated and observed. However, too much oxygen was found to significantly lower polymer MWs. An on–off control strategy is preferred over a continous feed system. The detrimental effect on product MW will limit the applicability of oxygen control to batch reactors. This aspect of

$T_{set\ pt.}$ \ O_2 set pt. (SCCM)	10	20	30	40	50	60
72	NC	NC	NC	46 NC t = 52min x = 88.5% $8.3\times10^6 \frac{gm}{gmole}$	44 C t = 60min x = 93.4% $7.7\times10^6 \frac{gm}{gmole}$	36 C t = 37.5min x = 91.3% $8.6\times10^6 \frac{gm}{gmole}$
70	NC	41 NC t = 50min x = 94.8% $7.8\times10^6 \frac{gm}{gmole}$	37 NC t = 40min x = 95.2% $6.6\times10^6 \frac{gm}{gmole}$	38 NC t = 40min x = 93.6% $7.1\times10^6 \frac{gm}{gmole}$	34 C t = 40min x = 92.7% $6.5\times10^6 \frac{gm}{gmole}$	33 C t = 40min x = 101.8% $6.5\times10^6 \frac{gm}{gmole}$
68	NC	40 NC t = 50min x = 99% $7.3\times10^6 \frac{gm}{gmole}$	39 C t = 40min x = 86.8% $7.3\times10^6 \frac{gm}{gmole}$	42 C t = 50min x = 93.5% $6.9\times10^6 \frac{gm}{gmole}$	C	32 C t = 57.5min x = 96.9% $6.5\times10^6 \frac{gm}{gmole}$
66	45 NC t = 55.5min x = 91.4% $5.3\times10^6 \frac{gm}{gmole}$	43 C t = 70min x = 89.4% $6.1\times10^6 \frac{gm}{gmole}$	C	C	C	C
64	C	21 C	C	C	C	20 C

UNCONTROLLED RUN 11.1×10^6 gm/gmole (t = 40min, x = 93.6%)
NEAR-ISOTHERMAL RUN (set pt. 60°C) 5.3×10^6 gm/gmole (t = 150min, x = 70.1%)
$O_{2\ set\ pt.}$ 55 SCCM

Fig. 11. Effect of proportional temperature (oxygen) control on the viscosity average molecular weight of PMMA produced by emulsion polymerization. The bold line delineates the boundary between control (C) and no control (NC) of the autoaccelerative gel effect. Emulsion experiment numbers are given in the upper left hand of corner of a grid square. $[M_0] = 3.75$ g mol/L H_2O, $[I_0] = 0.0037$ g mol/L H_2O, $[S_0] = 0.0347$ g mol/L H_2O, and $T_c = 60$°C. Run 31 had a set point of 62°C and max O_2 flow of 35 sccm.

oxygen control must be studied further, before actual application to continuous processes is implemented.

On the other hand, the use of oxygen control appears quite promising in view of the rapid response time. It can be readily employed to prevent reactor runaway and changes in steady state in CSTRs since the reaction can be inhibited almost immediately. Oscillatory particle nucleation can be controlled since the rate of polymerization can be easily manipulated. Whenever particles grow too fast, a pulse of oxygen can be injected and most reaction suppressed. Particle growth resumes as the dissolved oxygen is consumed. Further work (on an actual CSTR train) is needed to demonstrate the full potential of this kind of oxygen control.

References

1. J. L. Gardon, in *Applied Polymer Science*, J. K. Craver and R. W. Tess, Eds., ACS Organic Coatings and Plastics Chemistry, Am. Chem. Soc., New York, 1975.

2. J. Brandup and E. H. Immergut, Eds., *Polymer Handbook*, 2nd ed., Wiley-Interscience, New York, 1975.

3. I. M. Kolthoff and I. K. Miller, *J. Am. Chem. Soc.*, **73**, 3055 (1951).

4. H. J. James, Jr. and I. Piirma, *Am. Chem. Soc. Symp. Ser.*, **24**, 197 (1976).

5. N. Friis and A. E. Hamislee, *J. Polym. Sci. Polym. Chem. Ed.*, **12**, 251 (1974).

6. R. Patsiga, M. Litt, and V. Stannett, *J. Phys. Chem*, **64**, 801 (1960).

7. D. Lynch and C. Kiparissides, *J. Appl. Polym. Sci.*, **26**, 1283 (1981).

Received September 20, 1984
Accepted January 16, 1985